

OPEN ACCESS

**Repository of the Max Delbrück Center for Molecular Medicine (MDC)
in the Helmholtz Association**

<https://edoc.mdc-berlin.de/20298/>

**Increased angiotensin II formation in the brain modulates
cardiovascular homeostasis and erythropoiesis**

Rodrigues A.F., Todiras M., Qadri F., Campagnole-Santos M.J., Alenina N., Bader M.

The final version of record is available at

<https://portlandpress.com/clinsci/article/135/11/1353/228694/Increased-angiotensin-II-formation-in-the-brain>

This is a copy of the accepted manuscript, as originally published online ahead of print by Portland Press. The original article has been published in final edited form in:

Clinical Science
2021 JUN 02 ; 135(11): 1353-1367
2021 MAY 20 (first published online: final publication)
doi: [10.1042/CS20210072](https://doi.org/10.1042/CS20210072)

Publisher: [Portland Press](#)

Copyright © 2021 The Author(s). Published by Portland Press Limited on behalf of the
Biochemical Society

Increased angiotensin II formation in the brain modulates cardiovascular homeostasis and erythropoiesis

André Felipe Rodrigues^{1,2,3}, Mihail Todiras^{1,4}, Fatimunnisa Qadri¹, Maria Jose Campagnole-Santos⁵, Natalia Alenina^{1,3} & Michael Bader^{1,3,6,7,*}

¹Max-Delbrück-Center for Molecular Medicine, Berlin, Germany

²Department of Biology, Chemistry and Pharmacy, Free University of Berlin, Berlin, Germany

³German Center for Cardiovascular Research (DZHK), Partner Site Berlin, Germany

⁴Nicolae Testemițanu State University of Medicine and Pharmacy, Chisinau, Moldova

⁵Laboratory of Hypertension, Institute of Biological Sciences, Federal University of Minas Gerais, Belo Horizonte, Brazil.

⁶Charité Universitätsmedizin Berlin, Berlin, Germany

⁷Institute for Biology, University of Lübeck, Lübeck, Germany

*Corresponding Author: mbader@mdc-berlin.de

Abstract

In spite of the fact that the modulatory effects of angiotensin II (Ang II) on the sympathetic nerve activity to targeted organs involved in blood pressure (BP) regulation is well acknowledged, the local production of this peptide in the brain and the consequences of enhanced central Ang II beyond the cardiovascular system are not yet well comprehended. In this study, we generated and validated a new transgenic mouse line overexpressing the rat full-length angiotensinogen (Agt) protein specifically in the brain (Agt-Tg). Adult Agt-Tg mice presented overall increased gene expression of total Agt in the brain including brainstem and hypothalamus. In addition, the excess of Agt led to abundantly detectable brain Ang II levels as well as increased circulating copeptin levels. Agt-Tg displayed raised BP in acute recordings, while long-term telemetrically measured basal BP was indistinguishable from wildtypes. Agt-Tg has altered peripheral renin angiotensin system and vasomotor sympathetic tone homeostasis, because renal gene expression analysis, plasma Ang II measurements and ganglionic blockade experiments revealed suppressed renin expression, reduced Ang II and higher neurogenic pressure response, respectively. Plasma and urine screens revealed apparently normal fluid and electrolyte handling in Agt-Tg. Interestingly, hematological analyses showed increased hematocrit in Agt-Tg caused by enhanced erythropoiesis, which was reverted by submitting the transgenic mice to a long-term peripheral sympathectomy protocol. Collectively, our findings suggest that Agt-Tg is a valuable tool not only to study brain Ang II formation and its modulatory effects on cardiovascular homeostasis but also its role in erythropoiesis control via autonomic modulation.

Keywords: Brain RAS; Neurophysiology; Blood Pressure; Sympathetic System; Red Blood Cells

Introduction

The renin angiotensin system (RAS) is a major blood pressure (BP) and hydromineral balance regulator [1–3]. Acting on two receptor types (AT1 and AT2) with opposite effects, angiotensin II (Ang II) is the main effector peptide within the system. Among the effects exerted by Ang II are cardiac contractility, vasoconstriction, and renal sodium and water reabsorption directly or indirectly via aldosterone release [1,4]. At the brain level, Ang II regulates thirst, salt appetite, vasopressin release, as well as BP which is mainly controlled by changing the sympathetic nerve activity (SNA) to cardiovascular organs [1,3,5,6]. Altogether, these physiological actions of Ang II on different organs render it one of the most important hormones in BP control. Compelling evidence supports Ang II formation apart from the circulation directly in tissues, because the RAS precursor protein angiotensinogen (Agt) and the enzymes (renin and angiotensin converting enzyme) required for Ang II formation are expressed and/or imported from the circulation into some organs, especially the ones involved in cardiovascular control [1,3].

The brain differs from the peripheral cardiovascular organs because the blood-brain-barrier (BBB), at least in homeostatic conditions, limits the traffic of Ang II and other RAS components into the brain. Therefore, the majority of the neurophysiological effects modulated by Ang II must be exerted by brain-borne Ang II produced from the cleavage of the abundant astrocyte secreted Agt [7,8], with the exception of Ang II actions on the circumventricular organs where the BBB is permeable for the peptide [1,9,10]. However brain Ang II synthesis is still a matter of debate since there is very low brain renin expression and the truncated renin protein expressed in the brain accumulates in the cytosol with no access to Agt [9,10]. Besides that, no other enzyme has been so far conclusively proven to have renin-like activity or form Ang II directly from Agt in the brain. However, we showed that life-long antisense-RNA mediated knock down of *Agt* specifically in the brain of rats without affecting the circulating RAS led to BP reduction and diabetes insipidus due to reduced vasopressin release [7]. Additionally, this transgenic rat presented reduced BP responses to stress and exogenous administered Ang II, highlighting the dependence of locally produced brain Ang II in modulating SNA in both cases [11,12].

The rostral ventrolateral medulla (RVLM) is the main nodal point of SNA sorting and branch-specific activation. Ang II is an important differential SNA branch modulator, either directly binding to some of the RVLM neurons or indirectly modulating the firing of neuronal cells projecting to the RVLM [5,13,14]. Indeed, a distinct SNA branch activation was observed when different nerves were chronically recorded during Ang II-induced hypertension in rats [15,16]. Most of the studies investigating SNA modulation by brain Ang II in physiological and pathological conditions focused on the cardiovascular organs involved in BP control. However, also non-cardiovascular organs including the bone marrow and spleen as the main hematopoietic organs are densely innervated by the autonomic system [17–19]. Moreover, the elevation of brain Ang II content in rodents potentiates SNA to these organs [20,21], and growing evidence suggests an immunomodulatory role of brain Ang II via the autonomic system to these hematopoietic organs contributing to hypertension development and end-organ damage [17,19,20]. However, contrary to the immune cell modulation the modulatory effects of brain Ang II on erythropoiesis are not well documented.

In the present study, we developed and phenotyped a new transgenic mouse line life-long overexpressing rat Agt specifically in the brain. The model was used to verify the brain's ability to produce Ang II as well as to investigate its modulatory effects on basal cardiovascular, hydromineral and erythropoiesis homeostasis.

Material and Methods

Generation of FVB/N-*Tg(hGFAP-rAgt)24Bdr* (Agt-Tg)

We generated a new transgenic mouse line, FVB/N-*Tg(hGFAP-rAgt)24Bdr* (Agt-Tg), expressing the rat *Agt* in brain astrocytes the major cell type expressing *Agt* in the brain [7,8]. In these animals, the rat *Agt* is expressed under the control of the human glial fibrillary acidic protein (GFAP) promoter as previously successfully used in rodents [7,22,23]. Briefly, rat liver total RNA was isolated and a cDNA library prepared as described below. The rat *Agt* full-length cDNA (XM_008772597) was amplified by a PCR reaction with the following specific primers (5'-GGACACACAGAAGCAAGTCC-3' and 5'-CATGGCTACACAGGAGGCAT-3'). To generate Agt-Tg, a linear construct (Figure 1A) was prepared and used for pronuclear injection into fertilized nuclei of one-cell FVB/N mouse embryos. Positive founders and transgenic offspring were genotyped by PCR using the primers (5'-TGACACCAACCCCGAGTGG-3' and 5'-TCTGCCAGAAAGTGCAGCG-3') yielding a 190 bp transgene-specific PCR band.

Animals

For the generation of experimental animals, heterozygous Agt-Tg males were mated with wildtype FVB/N females and littermates were used. The mice were kept as 4-6 in each cage with free access to standard chow and water in a temperature controlled room 22±1°C under a light cycle of 12h:12h (light/dark). 13-20 week-old male mice were used for the experiments. The animal experiments were performed at the animal facility of the Max Delbrück Center for Molecular Medicine (Berlin) according to the EU directive 2010/63/EU for animal experiments. All animal experimental procedures were approved by the Berlin State Office for Health and Social Affairs (*Landesamt für Gesundheit und Soziales*, #G0316/18).

Cardiovascular parameter acquisition and *in vivo* drug treatments

Cardiovascular parameter recording: BP and heart rate (HR) were acquired in freely moving mice using two different methods: 1) saline-heparin filled catheter and 2) radio-

telemetry. In both methods, a small incision over the femoral triangle was made, the femoral artery and vein were isolated from surrounding tissue, and ligated permanently and temporary distally and proximally, respectively. The arterial catheters from method 1 and 2 were introduced into the femoral artery ~1.5 cm proximally to reach the abdominal aorta before the renal artery bifurcation. In method 1, another catheter was inserted into the femoral vein for drug administration. The self-made catheters from method 1 were subcutaneously tunneled and exteriorized at the interscapular region and were secured with a silk-suture 3/0 [24]. The bodies from the pressure transmitters PhysioTel (DSI #PA-C10) in method 2 were allocated into a subcutaneous pouch on the back. All mice received 200 mg/Kg/day metamizole in drinking water before and after surgery, and all surgical procedures were performed under ketamine and xylazine anesthesia (100 and 10 mg/Kg, respectively). After surgery and until the end of the cardiovascular data acquisition, the animals were housed individually. Catheter-filled data acquisition and drug-response protocols were performed 2 days after the surgery between ZT3 and ZT7 (3-7 hours after the onset of the light) in freely moving mice. At least one week before surgeries, mice were transferred to a quiet room, where the recordings were performed. The room temperature and light cycle were the same as previous. Baseline cardiovascular parameters were acquired before any drug protocol, beat-by-beat, for ~1 hour following a habituation period of ~1 hour, after connecting the mouse to the pressure transducer. To measure the arterial pulse waveform (systolic and diastolic), the arterial catheter was connected to a heparin/saline (100 U/ml) filled tube connected to a pressure transducer (AD Instruments #MLT0699) connected to a PowerLab/4sp via bridge amplifiers (AD Instruments #ML110). MAP was automatically calculated with the formula $MAP = [systolic + (2 * diastolic)] / 3$, and the HR estimated from the oscillatory pressure waveform. Data was acquired and analyzed using a computer system equipped with a LabChart v5 software (AD Instruments). Acute intravenous injections were performed after venous catheter flushing, and when the mouse displayed minimal activity. Radio-telemetry parameters (systolic and diastolic pressure, HR and locomotor activity) were first acquired 12-14 days after telemeter implantation with PhysioTel receivers (DSI #RPC-1) connected to a DSI data exchange matrix. Mice were placed in the experimental room after surgery and remained there during the whole habituation

and recording periods. Data was recorded 24 hours for 10 seconds every 5 minutes for 5 consecutive days and analyzed with the software Dataquest A.R.T. (DSI).

Neurogenic pressor activity: To verify the influence of the sympathetic tone on basal BP, freely moving mice instrumented with arterial and venous catheters received a single bolus injection of hexamethonium (20 mg/Kg, *iv*) and the peak depressor response was used as an index of vasomotor tone. Hexamethonium bromide (Sigma #H0879) was diluted in 0.9% physiological saline and injected in a final volume of 100 μ L (drug + saline to wash out).

Baroreflex control of the heart rate: Cardiac frequency responses to transient increases and decreases in MAP elicited by intravenous bolus injections of 5 μ g/Kg phenylephrine hydrochloride (Sigma #P1250000) and 10 μ g/Kg sodium nitroprusside (Sigma #71778), respectively, were recorded in freely moving mice. To calculate the baroreceptor sensitivity index, the MAP and HR peak responses to phenylephrine and sodium nitroprusside were recorded beat-by-beat. First, the basal and the peak response changes in the HR were converted to changes in pulse interval (PI, ms) by the formula 60.000/HR. The Δ PI was calculated using the formula (Δ PI = peak response PI - basal PI). Finally, the baroreflex sensitivity index was established with the formula (BRS = Δ PI/ Δ MAP, ms/mmHg).

Chemical sympathectomy: Peripheral sympathetic ablation was achieved administering 6-Hydroxydopamine hydrobromide (6-OHDA; Sigma #162957). 6-OHDA was freshly prepared in 0.9% physiological saline containing 0.01% ascorbic acid and injected at a dose of 100 mg/Kg *i.p* once a day for 5 consecutive days. The mice were sacrificed for hematological analyses 3 weeks after the last 6-OHDA injection.

Sample collection

All samples were collected between ZT5-ZT6 to match with the acute cardiovascular phenotyping and prevent circadian bias. Timed spontaneous urine was collected directly into a tube and snap frozen with dry ice, the procedure was repeated on the following

day, in case the mouse bladder was found empty. All mice were sacrificed with isoflurane vapor overdose followed by exsanguination. Fresh blood for hematological analyses was collected from cardiac puncture into MiniCollect[®] EDTA-K3 coated tubes (Greiner #450531). Plasma samples were prepared centrifuging at 2000 g 10 min 4°C blood collected into lithium-heparin tubes (Greiner #450537) or MiniCollect[®] EDTA-K3 coated tubes (Greiner #450531) for western blot. Brains used for in situ hybridization were removed from the skull rinsed in PBS and stored in 4% paraformaldehyde at room temperature until further processing. Whole brains used for Ang II measurements were collected immediately after the death of the mouse, and shortly rinsed in cold PBS to remove blood excess. To perform brain gene expression analyses, hypothalamus and brainstem were harvested *en bloc*, kidneys were removed and decapsulated. Several tissues (white fat, brain, adrenal gland, heart, spleen, kidney, bone marrow and liver) were harvested from Agt-Tg and wildtype mice to verify brain-specific transgene expression. All tissues used for gene expression and Ang II measurements were snap frozen in liquid nitrogen and stored at -80°C until the experiment.

In situ hybridization using RNAScope technology to localize the transgene mRNA combined with immunofluorescence staining of target protein

To locate the transgene (rat *Agt*) mRNA in Agt-Tg brain sections, in situ hybridization (ISH) using RNAScope technology was used. For ISH, mouse brains were fixed in 4% formalin and embedded in paraffin. Briefly, 5 µm brain sections were mounted on super frost glass slides and dried overnight at RT. The sections were then deparaffinized with xylene, rehydrated with a series of descending concentrations of ethanol, and air dried for 10 min. Brain sections were pretreated for ISH. Next, incubated with the RNAScope probe. Finally, the ISH signal was amplified using RNAScope[®] 2.5 HD Detection Reagents-RED (Advanced Cell Diagnostics #322360). Brain sections pretreatment, probe incubation and signal amplification were performed following manufacturer's instructions for RNAScope[®] 2.5 technique (Advanced Cell Diagnostics). A 20 ZZ-ISH probe targeting rat *Agt* mRNA was designed and synthesized by Advanced Cell Diagnostics (Rn-Agt-O1 #553841, Lot #20205A)

After developing the ISH chromogenic signal for rat *Agt* and prior to the immunofluorescence procedure, the sections were washed in distilled water and

incubated in PBS for 1h at RT. Then first, the sections were blocked with 10% normal donkey serum for 1h at RT. Second, the sections were overnight incubated with a primary polyclonal antibody anti-GFAP raised in guinea pig (GFAP, 1:500, Synaptic systems #173004) at 4°C in a wet chamber. In the next day, the sections were washed and incubated with fluorescent Alexa Fluor 488 conjugated secondary antibody anti-guinea pig (1:500, Jackson ImmunoResearch #706-545-148) in a wet chamber for 2h at RT. Subsequently, the slides were washed with PBS and cover slipped using Vectashield antifade mounting medium with DAPI (Vector Laboratories #H-1200-10). Finally, light microscopy and immunofluorescence images were made with an inverted microscope (Keyence #BZ-9000).

Qualitative and quantitative gene expression analyses

cDNA library preparation: Total RNA was extracted from ~100 mg tissue using the Trizol/chloroform method. Each tissue was homogenized in 1 ml of Trizol (Invitrogen #15596018) using a homogenization system (FastPrep; MPI #116004500). Possible remaining genomic DNA contamination was removed from 5 µg RNA using recombinant DNase I (Sigma, #04716728001). The cDNA was produced from 2 µg of DNase I treated RNA, using M-MLV reverse transcriptase (Promega #M170B) following manufacturer's instructions. Nucleic acid concentrations were quantified at each step using a NanoDrop (PepLab #ND-1000).

Qualitative organ specific transgene expression: Reverse transcription PCR (RT-PCR) was used to validate brain-specific transgene expression. The cDNA libraries produced from white fat, brain, adrenal gland, heart, spleen, kidney, bone marrow and liver were diluted to a final concentration of 20 ng/µL. Two separated PCRs were assembled with a Taq DNA Polymerase mix (NEB #M0267) and specific primers against the rat *Agt* (to identify transgene expression) (5'- CTGAGTGAGGCAAGAGGTGTA-3' and 5'- GCAGTCTCCCTCCTTCACAG -3'), and the mouse *Agt* (to identify endogenous expression) (5'- CTGAATGAGGCAGGAAGTGGG -3' and 5'- GCAGTCTCCCTCCTTCACAG -3'). The 150 bp amplicons were visualized loading and running the samples through a 2.5% agarose gel at 120 V for 30 minutes. Gels were imaged with a gel imager (Azure Biosystems #c200)

Quantitative gene expression analyses: Whole brain (half hemisphere), hypothalamus, brainstem and kidney cDNA were diluted to a final concentration of 1 ng/ μ l to perform quantitative reverse transcription PCR (RT-qPCR) experiments. RT-qPCR assays were assembled with a SYBR green reagent mix (Promega #A6002) following manufacturer's instructions. Specific primer sequences are: total *Agt* (rat and mice *Agt*) (5'-CCATTCAGGCCAAGACCTCC-3' and 5'-GCAGTCTCCCTCCTTCACAG-3'), mouse *Agt* (5'-CTGAATGAGGCAGGAAGTGGG-3' and 5'-GCAGTCTCCCTCCTTCACAG-3'), *Agtr1a* (5'-AAAGCCTGCGTCTTGTCTG-3' and 5'-TCGTGAGCCATTTAGTCCGA-3'), *Agtr1b* (5'-TGTGGGCAGTTTATACCGCT-3' and 5'-ACACTGGCGTAGAGGTTGAA-3'), *Agtr2* (5'-ATGATTGGCTTTTTGGACCTGT-3' and 5'-AAGGGTAGATGACCGATTGGT-3'), Renin (*Ren1d* and *Ren2*) (5'-CAAAGTCATCTTTGACACGGG-3' and 5'-AGTCAGAGGACTCATAGAGGC-3'), *Epo* (5'-ACTCTCCTTGCTACTGATTCCT-3' and 5'-ATCGTGACATTTTCTGCCTCC-3'), 18s (5'-TTGATTAAGTCCCTGCCCTTTGT-3' and 5'-CGATCCGAGGGCCTCACTA-3') and *Gapdh* (5'-TCACCACCATGGAGAAGGC-3' and 5'-GCTAAGCAGTTGGTGGTGC-3'). The gene expression analyses were carried out using a QuantStudio™ 5 device (Thermo Fischer #A28140). The Ct values obtained in the exponential phase of amplification from the gene of interest and the housekeeping genes 18s or *Gapdh* were used to calculate the relative gene expression to the control group (FVB/N) using the method of Livak and Schmittgen [25] ($2^{-\Delta\Delta CT}$).

Agt protein quantification

Whole brain (half hemisphere) and plasma *Agt* levels were estimated with western blots. Brain tissue was homogenized in RIPA buffer (100mg/mL, Abcam #ab156034) supplemented with a protease inhibitor cocktail (cOmplete™, Roche #COEDTAF-RO), and EDTA-plasma was diluted in distilled water (1:10, v/v). Total protein levels of brain and plasma were quantified with the BCA Assay (Sigma #BCA1-1KT). Previous to the electrophoresis, samples were mixed and boiled at 95 °C for 5 minutes in a reducing loading buffer based on the Laemmli formulation (1:4, v/v; Carl Roth #K929.1). 30 μ g of protein was loaded and separated by electrophoresis in a 10% polyacrylamide SDS-gel. Proteins were transferred to a nitrocellulose membrane using a Trans-Blot Turbo (Bio-

Rad #1704150). Membranes were blocked with a PBS based blocking solution (Intercept, LI-COR #927-70001) for 1 hour at room temperature. Subsequently, membranes were incubated overnight at 4 °C with a primary anti-Agt antibody raised in rabbit (Agt, 1:100; IBL #28101). This antibody binds to the C-terminal portion of both mouse and rat Agt, therefore, intact and des-AngI-Agt are recognized. Membranes were washed in (PBS-T; PBS plus 0.2% Tween-20), and incubated for 2 hours at room temperature with a secondary anti-rabbit conjugated-IRDye-800CW antibody (1:10000; LI-COR #926-32213). Membranes were washed in PBS and scanned using an Odyssey infrared imaging system (LI-COR #9120). The signals were analyzed using Image Studio Lite Software. Brain protein levels were normalized to Glyceraldehyde-3-phosphate dehydrogenase (GAPDH) following the protocol above. The primary and secondary antibodies are anti-GAPDH (GAPDH, 1:2000, Cell Signaling #2118) and anti-rabbit conjugated-IRDye-680RD (1:10000 LI-COR #926-68073), respectively. Plasma Agt levels were normalized to a total protein stain of the membrane with a commercial kit (LI-COR #926-11015) after protein transfer and before membrane blocking.

Ang II quantification

To quantify whole brain Ang I, Ang II, Ang III and Ang 1-7 levels, a LC-MS/MS approach was employed. The peptide quantification was carried out by Attoquant Diagnostics GmbH as described elsewhere [10]. Briefly, whole brains were homogenized in solution (ice-cold 6 M guanidine hydrochloride supplemented with 1% trifluoroacetic acid; 100 mg/ml), and before the LC-MS/MS the samples were spiked with a known concentration of stable isotope-labeled Ang II that was used as an internal control. The lower limit of detection for Ang I, Ang II and Ang III were 10 fmol/g, and 15 fmol/g for Ang 1-7.

Plasma Ang II levels were quantified by radioimmunoassay as described by Schelling et al. [26].

Plasma copeptin estimation

Plasma copeptin levels were estimated using an ELISA kit (RayBio #EIA-COP) following manufacturer's instructions.

Plasma clinical chemistry

Lithium-heparin plasma was used to quantify plasma levels of sodium, Na; potassium, K; glucose, GLC; total proteins, TP; albumin, ALB; creatinine, CRE; and urea. Blood urea nitrogen, BUN, was calculated from urea levels using the formula $BUN = (Urea \times 0.467)$. Plasma osmolarity was calculated with the formula $Osmolarity = \frac{[2(Na) + (GLC)]}{[18 + (BUN)/2.8]}$. The measurements were carried out by trained personnel at the animal phenotyping facility of the Max Delbrück Center for Molecular Medicine with an automated analyzer (Beckman Coulter #AU480).

Urine clinical chemistry

Timed urine was used to measure the concentrations of urinary Na, K, ALB and CRE. These parameters were measured with the same device used for the plasma chemistry. Because renal creatinine clearance throughout the day is constant [27], the measured urinary concentration of creatinine was used to estimate the urinary volume using inverse proportion and considering the control group average as 100%.

Blood hematology

EDTA blood was kept at room temperature to preserve cell morphology, and blood cell analyses was carried out with an automated hematology analyzer (IDEXX #ProCyte DX) within 4 hours after sampling at the animal phenotyping facility of the Max Delbrück Center for Molecular Medicine.

Capillary hematocrit

Blood collected into lithium-heparin tube was transferred to a hematocrit glass capillary (Hirschmann #9100275). The tubes were centrifuged at 13000 rpm for 10 minutes in a hematocrit centrifuge (Hettich #2010), and the percentage of red blood cells (RBC) was deduced from total volume measured with a digital caliper (Wabeco #11320).

Statistical Analyses

Data are presented as mean \pm SD unless stated otherwise in the figure legend. Statistical analyses were carried out using GraphPad Prism software. Data were analyzed using Student's *t* test or two-way ANOVA, as indicated. *Post hoc* analyses for

main effects and interactions were performed using the Tukey's test. In all analyses differences were considered statistically significant, whenever a $p < 0.05$ was identified.

Results

Generation and validation of the transgenic mouse model with brain specific *Agt* overexpression

A DNA construct coding for rat *Agt* under control of the human GFAP promoter (Figure 1A) was microinjected into FVB/N mouse zygotes to generate transgenic animals, a positive founder was identified and the line *Agt*-Tg was established mating this mouse. *Agt*-Tg males and females are born in normal Mendelian ratios, grow normally, and are fertile. Additionally, no apparent alteration was observed at gross morphological inspection of *Agt*-Tg. The brain-specificity of transgene expression was validated by RT-PCR with mRNA from different organs and a specific primer pair against rat *Agt* (Figure 1B). In parallel, we performed another PCR reaction with the same samples using specific primers against mouse *Agt* and confirmed the endogenous expression in liver and brain (Figure 1B). To assess the cellular localization (astrocyte) of transgene expression in the brain, we combined RNAScope for rat *Agt* with immunofluorescence staining with an antibody against the mouse GFAP protein. Figure 1C shows abundant transgene expression in GFAP positive cells, demonstrating successful astrocyte-specific transgene expression. Using the RNAScope technology, the transgene expression was found wide-spread across different brain regions including the paraventricular nucleus of the hypothalamus (Figure 2A) and the brainstem (Supplementary Figure 1).

RT-qPCR was used to quantify the total *Agt* expression (mouse and rat) in whole brain and key brain regions for cardiovascular control. Total *Agt* mRNA was found increased in the whole brain (Figure 2B) as well as in the hypothalamus (Figure 2C) and brainstem (Figure 2D) of *Agt*-Tg. Regarding mouse *Agt* expression wildtype and *Agt*-Tg displayed similar levels, indicating a non-suppressive effect of the transgene on the mouse endogenous *Agt* gene (Supplementary Figure 2A-C). Accordingly, total *Agt* protein levels were increased in *Agt*-Tg brains (Figure 2F). In addition, we measured the hypothalamic expression of all three Ang II receptors in the mouse but no evident differences between wildtype and *Agt*-Tg were found (Supplementary Figure 2D-F). After confirming increased total *Agt* expression across the brain including brain regions containing cardiovascular centers in *Agt*-Tg, we measured Ang II in whole brains of *Agt*-

Tg. Ang II was not detectable in the brains of wildtype mice but it was detected in the brains of Agt-Tg (Figure 2E), suggesting local brain production of the peptide due to increased substrate availability. In contrast, Ang I, Ang III and Ang 1-7 were not detected in brain samples of wildtype and Agt-Tg mice.

Vasopressin release in Agt-Tg

Vasopressin release into the bloodstream is known to be potentiated by brain Ang II. Therefore, we measured the plasma levels of copeptin, a surrogate marker of vasopressin [28], as a functional read-out for increased brain Ang II. Figure 2J shows increased circulating copeptin levels in Agt-Tg.

Cardiovascular homeostasis in Agt-Tg

Agt-Tg displayed increased mean arterial pressure (MAP) acutely measured by arterial catheter (Figure 3A). However, basal MAP was not altered when evaluated over a period of 5 days in mice implanted with telemeters (Figure 3C). The HR was found at similar range in both measurements (Figure 3B,D). Also, locomotor activity (LA) estimated in the telemetry experiment was similar between wildtype and Agt-Tg mice (Figure 3E). Circadian oscillations of MAP, HR, and LA were not different in Agt-Tg (Figure 3F and Supplementary Table 1). Because brain Ang II may increase BP by potentiating SNA, including to the vasculature, we measured the BP drop induced by the ganglionic blocker hexamethonium (20 mg/Kg, *iv*) as a marker of sympathetic vasomotor tone. Strikingly, Agt-Tg responded with higher intensity to hexamethonium (Figure 3G) indicating increased SNA in these animals. Interestingly, Agt-Tg had normal plasma Agt protein levels (Figure 2G), reduced renal renin gene expression (Figure 2H), and reduced circulating Ang II (Figure 2I). Most likely this suppressed peripheral RAS compensated the effects of increased vasopressin and vascular SNA. Finally, we measured the baroreceptor sensitivity of the HR reflex using drug-induced increase and decrease in MAP. Agt-Tg displayed impaired baroreflex sensitivity to drug-induced bradycardia (Figure 3H) and tachycardia (Figure 3I). The pressor and depressor responses induced by phenylephrine and sodium nitroprusside, respectively, were similar between wildtype and Agt-Tg but the bradycardia and tachycardia responses to these drugs were blunted in Agt-Tg (Supplementary Table 2).

Hydromineral balance in Agt-Tg

To know if increased levels of brain Ang II alters the basal fluid and electrolyte homeostasis in Agt-Tg, we investigated the plasmatic and urinary markers displayed in Table 1. Agt-Tg exhibited apparently normal mineral excretion. The plasmatic and urinary levels of sodium and potassium were similar between wildtype and Agt-Tg mice. In addition, renal and muscular function markers were normal in Agt-Tg plasma (urea and creatinine) and urine (albumin). Interestingly, the estimated urinary volume was comparable in both lines because the urinary creatinine, a metabolite excreted at a constant rate, was not different between wildtype and Agt-Tg mice. Finally, we calculated blood osmolarity of Agt-Tg which was not different from wildtype littermates. Altogether these data do not only reveal normal renal function and fluid intake in Agt-Tg but also strongly support normal blood volume in the transgenic mice, because plasma parameters sensitive to hydration status like sodium, total proteins, albumin and the osmolality are normal in Agt-Tg (Table 1).

Erythropoiesis in Agt-Tg

The hematocrit of Agt-Tg was found increased in an initial experiment using glass capillary-based quantification (Figure 4A). As indicators of dehydration that may reduce the plasma volume leading to increased hematocrit were not altered in Agt-Tg (see above), we decided to further explore this phenotype in depth using an automated blood cell counter. Initially, we confirmed that increased brain Ang II led to enhanced red blood cell (RBC) counts in Agt-Tg (Figure 4B). Accordingly, an increased absolute hemoglobin concentration was observed (Figure 4C), despite normal hemoglobin amount *per* RBC (Figure 4E). Additionally the absolute numbers of reticulocytes, circulating RBC precursors, were also increased (Figure 4F) revealing that brain Ang II led to a potentiation of erythropoiesis in the transgenic mice. We suspected increased erythropoietin production could be the source of the increased erythropoiesis in the Agt-Tg mice, but gene expression analyses of renal erythropoietin did not reveal alterations in the animals (Figure 4D). Thus, we sought to ablate the peripheral sympathetic nervous system with 6-OHDA to test if brain-borne Ang II increases erythropoiesis via

SNA modulation. Remarkably, the RBC and hemoglobin values became equal in sympathectomized wildtype and Agt-Tg mice (Figure 4B,C). Moreover, reticulocyte production was comparable in wildtype and Agt-Tg mice after SNA ablation (Figure 4F). Altogether, the data strongly supports that Ang II via the SNA positively modulates erythropoiesis. In addition, no changes in white blood cells and platelets were detected at baseline between the two groups. However, the sympathectomy protocol depleted the circulating white blood cells to a similar extent in both wildtype and Agt-Tg (Supplementary Table 3).

Discussion

The phenotyping of Agt-Tg mice revealed and confirmed important aspects of the controversial brain Ang II generation and function. To our knowledge, this is the first report demonstrating *in vivo* brain Ang II production simply by increasing local *Agt* expression using transgenic technology. Accordingly, the localization of Ang II overproduction should depend on the still elusive enzyme(s) metabolizing Agt in the brain. We can not exclude that the relatively high concentrations of brain Ang II found in Agt-Tg exceed physiological levels but the model opens opportunities to uncover the metabolic pathway(s) responsible for local brain Ang II generation in future studies. Moreover, it allowed us to confirm known cardiovascular actions of central Ang II and to unravel novel effects of the brain peptide on erythropoiesis.

Despite BP was only altered during acute measurements, we could identify a new set point of BP homeostasis depending on the actions of brain Ang II and characterized by increased vasopressin (copeptin) release and SNA-induced vasomotor tone as well as suppressed peripheral RAS. Interestingly, Agt-Tg mice present normal fluid and electrolyte balance. Finally, this novel transgenic mouse model turned out to be a suitable tool to gain insights in the influence of brain Ang II on erythropoiesis which was found stimulated by brain Ang II via SNA.

The BBB isolates the peripheral from the local brain RAS. Indeed, Ang II does not reach brain areas within the BBB in homeostatic conditions [29]. In this scenario, any local actions of brain Ang II should be a product of brain-borne Ang II [1,9]. The low

brain renin expression and the fact that most of it remains cytosolic within neuronal cells, renders an interaction with the astrocyte and secretory vesicle-specific RAS precursor protein Agt unlikely [8], even inside of some neurons expressing *Agt* which are located at cardiovascular centers such as the RVLM [3]. Accordingly, the specific knockout of the intracellular renin isoform led to increased active phase hypertension in mice [30]. Despite that mass-spectrometry based Ang II quantification failed to identify Ang II peptide in brain samples of rodents [10], we could demonstrate reduced BP, vasopressin secretion and stress-induced BP response in rats with lifelong depleted brain Agt protein [7,12]. Other transgenic models provided further evidence of brain Ang II production and functionality, including a mouse model overexpressing the rat Ang II AT1a receptors in neurons and a mouse model with increased brain angiotensin converting enzyme 2. In both models, basal BP was not altered, but the baseline BP dependence on brain Ang II was increased, and autonomic dysfunction was improved during induced hypertension, respectively [31,32]. Besides that, many studies that blocked the brain RAS or increased it either using transgenic rodents or directly infusing Ang II into the brain showed potentiated neurogenic pressor response and metabolic alterations modulated by SNA in physiology and pathology [23,33–36].

Several rodent models successfully increased brain Ang II levels, among them are direct brain injections of Ang II, and transgenic models like the TGM(rTon) and the sRA. The first transgenic model is a mouse expressing the rat tonin in the brain leading to Ang II formation directly from Agt [23]. The second model is a double transgenic mouse carrying the human renin gene under a neuron specific promoter control, and human *Agt* with its own promoter [37]. In this model, the human *Agt* cleavage only happens via the human renin, because of the inability of mouse renin to metabolize human *Agt*. Even though these models added crucial knowledge to the field of brain Ang II research that revealed effects on the cardiovascular, metabolic and immune systems [20,23,33,37], they were not suitable to confirm endogenous Ang II formation in the brain. Agt-Tg allowed us to demonstrate for the first time the brain's ability to produce Ang II *in vivo*, because in the presented model Ang II was very likely produced via its natural pathway by simply increasing the availability of the precursor protein Agt instead of the enzymes involved in its metabolism.

After finding increased brain Ang II levels in Agt-Tg, the expected cardiovascular outcome is hypertension as previously demonstrated using intracerebroventricular Ang II infusions and other transgenic models [3,23,33,37,38]. However, comparisons of the cardiovascular phenotype among different transgenic models should be carefully interpreted because variables which are not always possible to control such as Ang II levels and location may deeply influence the final phenotype. Agt-Tg presented increased BP only in acute BP recording, during telemetry measurements no evident cardiovascular alterations were observed. This BP phenotype is not unprecedented because during the acute BP recording conditions the animal is presumably exposed to higher levels of stress, and brain Ang II is known to potentiate the SNA-dependent stress-induced BP response [12,34]. If the preexisting elevated Ang II levels potentiate the stress response or stress stimuli further raise brain Ang II formation to a level exceeding the normotensive limit in Agt-Tg remains elusive.

Agt-Tg revealed major alterations in components that are regulated by brain Ang II and may influence long-term BP regulation including activated SNA and increased vasopressin release [1,6,16,39]. Agt-Tg presented these alterations along with a reduced peripheral RAS most likely as compensatory response to increased BP. Additionally, Agt-Tg showed a blunted baroreflex control of HR. It is well established that acute Ang II actions on neurons at the nucleus tractus solitarii (NTS) that receives the afferent input impair the baroreceptor induced response by downregulating parasympathetic and sympathetic tone to the heart [40,41]. The role of chronically increased brain Ang II on the baroreflex control of the HR is, however, controversial. While some studies reported blunted function others reported a normal one due to reflex resetting [31,38,42,43]. Chronic heart failure blunts baroreflex sensitivity of HR and brain Ang II appears to be a major mediator of this process [44]. Again one should be aware that differences may arise when comparing different species and/or levels of brain Ang II in the different models.

Bone marrow and spleen, the main sources of the adult rodent erythrocytes in physiological or pathological conditions [45,46], receive dense autonomic innervation, and brain Ang II infusion increases SNA to these organs [17,20]. Also, norepinephrine, the main effector neurotransmitter in SNA, is recognized by several studies to stimulate bone marrow hematopoietic stem and progenitor cell migration into the circulation

[19,47,48]. The hormone erythropoietin which is mainly produced by renal cortical fibroblasts boosts erythropoiesis by favoring erythrocytic progenitor cell proliferation, differentiation and survival [49]. The elevated brain Ang II led to a SNA-dependent increase in erythropoiesis in Agt-Tg. Peripheral sympathectomy ablated the influence of SNA on erythropoiesis thereby reducing Agt-Tg RBC to levels comparable to controls. A previous study using the sRA double transgenic model with increased brain Ang II also reported increased hematocrit as our present study, but because this model presents an altered fluid intake the authors interpreted the phenotype as caused by dehydration [37]. Agt-Tg mice did not show obvious signs of disturbed fluid balance because their urinary output is normal along with plasma dehydration sensitive parameters (sodium, total proteins, albumin and osmolality), ruling out the possibility of increased RBC counts in Agt-Tg as consequence of dehydration-induced plasma volume reduction.

In summary, we have generated a new transgenic mouse model expressing rat *Agt* exclusively in the brain. The overall brain *Agt* elevation led to detectable Ang II levels in the brain of the transgenic mice supporting local Ang II synthesis. As consequence of higher brain levels of Ang II, BP was raised in acute recordings along with alteration in hormonal systems controlling BP homeostasis. Finally, we demonstrated that the brain-borne Ang II potentiates erythropoiesis via a SNA dependent mechanism.

Clinical perspectives

- The sympathetic nervous system is recognized as the major long-term blood pressure regulator, and angiotensin II positively modulates sympathetic nerve activity. However, local brain angiotensin II generation is not yet fully comprehended, but would open new therapeutic strategies to manage sympathetic-dependent disorders.
- The brain generates fully functional angiotensin II though current methodologies do not always detect the peptide in preclinical models. Brain angiotensin II disturbs blood pressure homeostasis and increases erythropoiesis via sympathetic nerve activity.
- Renin angiotensin system blockers are a first line therapy to treat hypertension. Towards improving personalized health, the blood brain barrier penetrance of substances should be taken into account not only to treat hypertension but also other sympathetic dysfunctions.

Data Availability

The data that support the findings of this study are available from the corresponding author upon reasonable request.

Competing Interests

The authors declare that there are no competing interests associated with the publication.

Funding

This work was supported by the German Research Foundation (DFG SFB1365) to NA and MB and a PROBRAL grant of CAPES/DAAD to MB and MJC.

Acknowledgments

We thank Andrea Rodak and Ilona Kamer for technical assistance.

References

- 1 Bader, M. (2010) Tissue Renin-Angiotensin-Aldosterone Systems: Targets for Pharmacological Therapy. *Annu. Rev. Pharmacol. Toxicol.* **50**, 439–465, 10.1146/annurev.pharmtox.010909.105610.
- 2 Yamazaki, O., Ishizawa, K., Hirohama, D., Fujita, T., and Shibata, S. (2019) Electrolyte transport in the renal collecting duct and its regulation by the renin–angiotensin–aldosterone system. *Clin. Sci.* **133**, 75–82, 10.1042/CS20180194.
- 3 Nakagawa, P., Gomez, J., Grobe, J. L., and Sigmund, C. D. (2020) The Renin-Angiotensin System in the Central Nervous System and Its Role in Blood Pressure Regulation. *Curr. Hypertens. Rep.* **22**, 7, 10.1007/s11906-019-1011-2.
- 4 Santos, R. A. S., Oudit, G. Y., Verano-Braga, T., Canta, G., Steckelings, U. M., and Bader, M. (2019) The renin-angiotensin system: going beyond the classical paradigms. *Am. J. Physiol. Heart Circ. Physiol.* **316**, H958–H970, 10.1152/ajpheart.00723.2018.
- 5 Guyenet, P. G. (2006) The sympathetic control of blood pressure. *Nat. Rev. Neurosci.* **7**, 335–346, 10.1038/nrn1902.
- 6 Llorens-Cortes, C. and Touyz, R. M. (2020) Evolution of a New Class of Antihypertensive Drugs. *Hypertension* **75**, 6–15, 10.1161/HYPERTENSIONAHA.119.12675.
- 7 Schinke, M., Baltatu, O., Bohm, M., Peters, J., Rascher, W., Bricca, G., et al. (1999) Blood pressure reduction and diabetes insipidus in transgenic rats deficient in brain angiotensinogen. *Proc. Natl. Acad. Sci.* **96**, 3975–3980, 10.1073/pnas.96.7.3975.
- 8 Stornetta, R., Hawelu-Johnson, C., Guyenet, P., and Lynch, K. (1988) Astrocytes synthesize angiotensinogen in brain. *Science.* **242**, 1444–1446, 10.1126/science.3201232.
- 9 Uijl, E., Ren, L., and Danser, A. H. J. (2018) Angiotensin generation in the brain: a re-evaluation. *Clin. Sci.* **132**, 839–850, 10.1042/CS20180236.
- 10 Van Thiel, B. S., Góes Martini, A., Te Riet, L., Severs, D., Uijl, E., Garrelds, I. M., et al. (2017) Brain Renin-Angiotensin System Does It Exist? *Hypertension* **69**, 1136–1144, 10.1161/HYPERTENSIONAHA.116.08922.

- 11 Baltatu, O., Silva, J. A., Ganten, D., and Bader, M. (2000) The Brain Renin-Angiotensin System Modulates Angiotensin II–Induced Hypertension and Cardiac Hypertrophy. *Hypertension* **35**, 409–412, 10.1161/01.HYP.35.1.409.
- 12 Baltatu, O., Campos, L. A., and Bader, M. (2004) Genetic targeting of the brain renin-angiotensin system in transgenic rats: Impact on stress-induced renin release. *Acta Physiol. Scand.* **181**, 579–584, 10.1111/j.1365-201X.2004.01333.x.
- 13 Guyenet, P. G., Stornetta, R. L., Souza, G. M. P. R., Abbott, S. B. G., and Brooks, V. L. (2020) Neuronal Networks in Hypertension. *Hypertension* **76**, 300–311, 10.1161/HYPERTENSIONAHA.120.14521.
- 14 Guyenet, P. G., Stornetta, R. L., Holloway, B. B., Souza, G. M. P. R., and Abbott, S. B. G. (2018) Rostral Ventrolateral Medulla and Hypertension. *Hypertension* **72**, 559–566, 10.1161/HYPERTENSIONAHA.118.10921.
- 15 Yoshimoto, M., Miki, K., Fink, G. D., King, A., and Osborn, J. W. (2010) Chronic Angiotensin II Infusion Causes Differential Responses in Regional Sympathetic Nerve Activity in Rats. *Hypertension* **55**, 644–651, 10.1161/HYPERTENSIONAHA.109.145110.
- 16 Osborn, J. W., Fink, G. D., and Kuroki, M. T. (2011) Neural Mechanisms of Angiotensin II–Salt Hypertension: Implications for Therapies Targeting Neural Control of the Splanchnic Circulation. *Curr. Hypertens. Rep.* **13**, 221–228, 10.1007/s11906-011-0188-9.
- 17 Carnevale, D. (2020) Neural Control of Immunity in Hypertension: Council on Hypertension Mid Career Award for Research Excellence, 2019. *Hypertension* **76**, 622–628, 10.1161/HYPERTENSIONAHA.120.14637.
- 18 Hanoun, M., Maryanovich, M., Arnal-Estapé, A., and Frenette, P. S. (2015) Neural Regulation of Hematopoiesis, Inflammation, and Cancer. *Neuron* **86**, 360–373, 10.1016/j.neuron.2015.01.026.
- 19 Ahmari, N., Hayward, L. F., and Zubcevic, J. (2020) The importance of bone marrow and the immune system in driving increases in blood pressure and sympathetic nerve activity in hypertension. *Exp. Physiol.* **105**, 1815–1826, 10.1113/EP088247.
- 20 Ahmari, N., Santisteban, M. M., Miller, D. R., Geis, N. M., Larkin, R., Redler, T., et al. (2019) Elevated bone marrow sympathetic drive precedes systemic

- inflammation in angiotensin II hypertension. *Am. J. Physiol. Circ. Physiol.* **317**, H279–H289, 10.1152/ajpheart.00510.2018.
- 21 Ganta, C. K., Lu, N., Helwig, B. G., Blecha, F., Ganta, R. R., Zheng, L., et al. (2005) Central angiotensin II-enhanced splenic cytokine gene expression is mediated by the sympathetic nervous system. *Am. J. Physiol. Circ. Physiol.* **289**, H1683–H1691, 10.1152/ajpheart.00125.2005.
- 22 Brenner, M., Kisseberth, W., Su, Y., Besnard, F., and Messing, A. (1994) GFAP promoter directs astrocyte-specific expression in transgenic mice. *J. Neurosci.* **14**, 1030–1037, 10.1523/JNEUROSCI.14-03-01030.1994.
- 23 Cardoso, C. C., Alenina, N., Ferreira, A. J., Qadri, F., Lima, M. P., Gross, V., et al. (2010) Increased blood pressure and water intake in transgenic mice expressing rat tonin in the brain. *Biol. Chem.* **391**, 435–441, 10.1515/BC.2010.040.
- 24 Todiras, M., Alenina, N., and Bader, M. (2017) Evaluation of Endothelial Dysfunction In Vivo. In *Methods in Molecular Biology*, pp 355–367.
- 25 Livak, K. J. and Schmittgen, T. D. (2001) Analysis of Relative Gene Expression Data Using Real-Time Quantitative PCR and the 2- $\Delta\Delta$ CT Method. *Methods* **25**, 402–408, 10.1006/meth.2001.1262.
- 26 Schelling, P., Ganten, U., Sponer, G., Unger, T., and Ganten, D. (1980) Components of the Renin-Angiotensin System in the Cerebrospinal Fluid of Rats and Dogs with Special Consideration of the Origin and the Fate of Angiotensin II. *Neuroendocrinology* **31**, 297–308, 10.1159/000123092.
- 27 Johnston, J. G. and Pollock, D. M. (2018) Circadian regulation of renal function. *Free Radic. Biol. Med.* **119**, 93–107, 10.1016/j.freeradbiomed.2018.01.018.
- 28 Christ-Crain, M. and Fenske, W. (2016) Copeptin in the diagnosis of vasopressin-dependent disorders of fluid homeostasis. *Nat. Rev. Endocrinol.* **12**, 168–176, 10.1038/nrendo.2015.224.
- 29 Biancardi, V. C., Son, S. J., Ahmadi, S., Filosa, J. A., and Stern, J. E. (2014) Circulating Angiotensin II Gains Access to the Hypothalamus and Brain Stem During Hypertension via Breakdown of the Blood–Brain Barrier. *Hypertension* **63**, 572–579, 10.1161/HYPERTENSIONAHA.113.01743.
- 30 Shinohara, K., Liu, X., Morgan, D. A., Davis, D. R., Sequeira-Lopez, M. L. S., Cassell, M. D., et al. (2016) Selective Deletion of the Brain-Specific Isoform of

- Renin Causes Neurogenic Hypertension. *Hypertension* **68**, 1385–1392, 10.1161/HYPERTENSIONAHA.116.08242.
- 31 Feng, Y., Xia, H., Cai, Y., Halabi, C. M., Becker, L. K., Santos, R. A. S., et al. (2010) Brain-Selective Overexpression of Human Angiotensin-Converting Enzyme Type 2 Attenuates Neurogenic Hypertension. *Circ. Res.* **106**, 373–382, 10.1161/CIRCRESAHA.109.208645.
- 32 Lazartigues, E., Dunlay, S. M., Loihl, A. K., Sinnayah, P., Lang, J. A., Espelund, J. J., et al. (2002) Brain-selective overexpression of angiotensin (AT1) receptors causes enhanced cardiovascular sensitivity in transgenic mice. *Circ. Res.* **90**, 617–624, 10.1161/01.RES.0000012460.85923.F0.
- 33 Leenen, F. H. H. (2014) Actions of Circulating Angiotensin II and Aldosterone in the Brain Contributing to Hypertension. *Am. J. Hypertens.* **27**, 1024–1032, 10.1093/ajh/hpu066.
- 34 de Kloet, A. D., Wang, L., Pitra, S., Hiller, H., Smith, J. A., Tan, Y., et al. (2017) A Unique “Angiotensin-Sensitive” Neuronal Population Coordinates Neuroendocrine, Cardiovascular, and Behavioral Responses to Stress. *J. Neurosci.* **37**, 3478–3490, 10.1523/JNEUROSCI.3674-16.2017.
- 35 Ko, S.-H., Cao, W., and Liu, Z. (2010) Hypertension management and microvascular insulin resistance in diabetes. *Curr. Hypertens. Rep.* **12**, 243–51, 10.1007/s11906-010-0114-6.
- 36 Kamitani, A., Higashimori, K., Kohara, K., Higaki, J., Mikami, H., and Ogihara, T. (1994) The effects of central administration of angiotensin II type-1 receptor antagonist, CV-11974, in nephrectomized spontaneously hypertensive rats. *Clin. Exp. Pharmacol. Physiol.* **21**, 271–6, 10.1111/j.1440-1681.1994.tb02512.x.
- 37 Grobe, J. L., Grobe, C. L., Beltz, T. G., Westphal, S. G., Morgan, D. A., Xu, D., et al. (2010) The Brain Renin-Angiotensin System Controls Divergent Efferent Mechanisms to Regulate Fluid and Energy Balance. *Cell Metab.* **12**, 431–442, 10.1016/j.cmet.2010.09.011.
- 38 Sharma, N. M., Haibara, A. S., Katsurada, K., Nandi, S. S., Liu, X., Zheng, H., et al. (2021) Central Ang II (Angiotensin II)-Mediated Sympathoexcitation. *Hypertension* **77**, 147–157, 10.1161/HYPERTENSIONAHA.120.16002.
- 39 Littlejohn, N. K., Siel, R. B., Ketsawatsomkron, P., Pelham, C. J., Pearson, N. A.,

- Hilzendeger, A. M., et al. (2013) Hypertension in mice with transgenic activation of the brain renin-angiotensin system is vasopressin dependent. *Am. J. Physiol. Integr. Comp. Physiol.* **304**, R818–R828, 10.1152/ajpregu.00082.2013.
- 40 Polson, J. W., Dampney, R. A. L., Boscan, P., Pickering, A. E., and Paton, J. F. R. (2007) Differential baroreflex control of sympathetic drive by angiotensin II in the nucleus tractus solitarii. *Am. J. Physiol. Regul. Integr. Comp. Physiol.* **293**, R1954–R1960, 10.1152/ajpregu.00041.2007.
- 41 Tan, P. S. P., Killinger, S., Horiuchi, J., and Dampney, R. A. L. (2007) Baroreceptor reflex modulation by circulating angiotensin II is mediated by AT1 receptors in the nucleus tractus solitarius. *Am. J. Physiol. Regul. Integr. Comp. Physiol.* **293**, R2267–78, 10.1152/ajpregu.00267.2007.
- 42 Sakai, K., Chapleau, M. W., Morimoto, S., Cassell, M. D., and Sigmund, C. D. (2004) Differential modulation of baroreflex control of heart rate by neuron- vs. glia-derived angiotensin II. *Physiol. Genomics* **20**, 66–72, 10.1152/physiolgenomics.00168.2004.
- 43 Gaudet, E., Godwin, S. J., and Head, G. A. (2000) Effects of central infusion of ANG II and losartan on the cardiac baroreflex in rabbits. *Am. J. Physiol. Circ. Physiol.* **278**, H558–H566, 10.1152/ajpheart.2000.278.2.H558.
- 44 Zucker, I. H., Xiao, L., and Haack, K. K. V. (2014) The central renin–angiotensin system and sympathetic nerve activity in chronic heart failure. *Clin. Sci.* **126**, 695–706, 10.1042/CS20130294.
- 45 Bozzini, C., Barrio Rendo, M., Devoto, F., and Epper, C. (1970) Studies on medullary and extramedullary erythropoiesis in the adult mouse. *Am. J. Physiol. Content* **219**, 724–728, 10.1152/ajplegacy.1970.219.3.724.
- 46 Pantel, K., Loeffler, M., Bungart, B., and Wichmann, H. E. (1990) A mathematical model of erythropoiesis in mice and rats. Part 4: Differences between bone marrow and spleen. *Cell Prolif.* **23**, 283–297, 10.1111/j.1365-2184.1990.tb01125.x.
- 47 Ho, Y.-H. and Méndez-Ferrer, S. (2020) Microenvironmental contributions to hematopoietic stem cell aging. *Haematologica* **105**, 38–46, 10.3324/haematol.2018.211334.
- 48 Méndez-Ferrer, S., Lucas, D., Battista, M., and Frenette, P. S. (2008)

Haematopoietic stem cell release is regulated by circadian oscillations. *Nature* **452**, 442–447, 10.1038/nature06685.

- 49 Jelkmann, W. (2011) Regulation of erythropoietin production. *J. Physiol.* **589**, 1251–1258, 10.1113/jphysiol.2010.195057.

Legend of Figures

Figure 1 - Generation of Agt-Tg

Schematic representation of the construct used to generate Agt-Tg (A). Organ specific transgenic rat *Agt* expression, top panel (B), and organ specific expression of the mouse endogenous *Agt*, bottom panel (B). Transgene mRNA localization in GFAP positive cells, ISH using RNAScope against rat *Agt* (red) combined with immunostaining against GFAP protein (green) in Agt-Tg brain, nuclei were counterstained with DAPI (blue) (C). Scale bar = 50 μm (magnification $\times 40$). WT = wildtype, Tg = Agt-Tg, Wf = white fat, Br = brain, Ad = adrenal gland, He = heart, Sp = spleen, Ki = kidney, Bm = bone marrow, Li = liver. R.Li = rat liver = positive control for the transgene PCR, H₂O = negative control for both PCRs.

Figure 2 – Brain gene expression, Ang II generation and copeptin release

Chromogenic visualization of transgene expression by RNAScope (red dots) in an Agt-Tg brain section showing the paraventricular nucleus of the hypothalamus (PVN) (A), nuclei were counterstained with hematoxylin. Increased total (rat and mouse) *Agt* (tAgt) mRNA expression in whole brain (B), hypothalamus (C) and brainstem (D) of Agt-Tg. Detectable high levels of Ang II in brains of Agt-Tg (E). Increased tAgt protein levels in brains of Agt-Tg (F). Unaltered plasma Agt protein levels in Agt (G). Decreased renal expression of renin (H), and plasma levels of Ang II (I) in Agt-Tg. Increased circulating plasma levels of copeptin in Agt-Tg (J). Scale bar = 500 μm (magnification $\times 2$); Scale bar = 50 μm (magnification $\times 20$). Values are mean \pm SD for 3-6 animals in each group. ** $p < 0.01$; *** $p < 0.001$; **** $p < 0.0001$ different from the FVB/N group (Student's *t* test). *n.d* = not detected. The dotted line in (E) represents the minimum detection limit of 10 fmol/g.

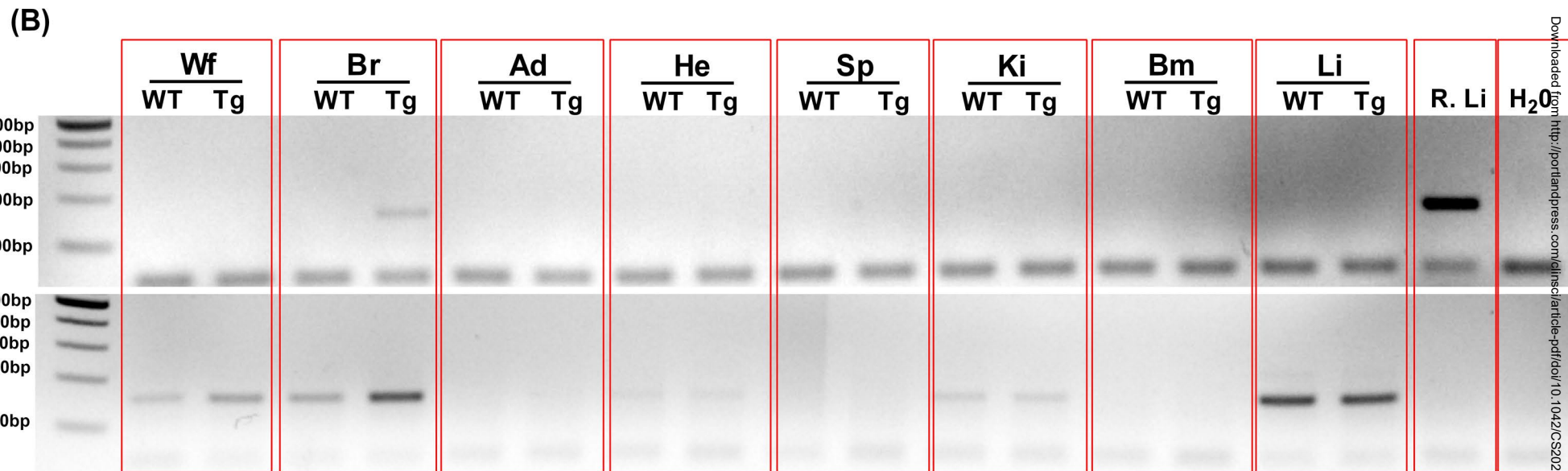
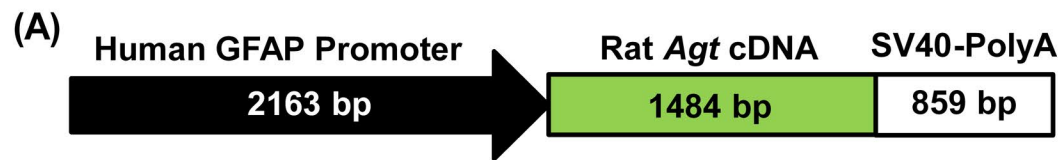
Figure 3 – Cardiovascular homeostasis in Agt-Tg

Increased MAP in freely-moving Agt-Tg acutely recorded with saline-heparin filled catheter (A), and normal MAP measured by radio-telemetry (5 days 24 hours averaged)

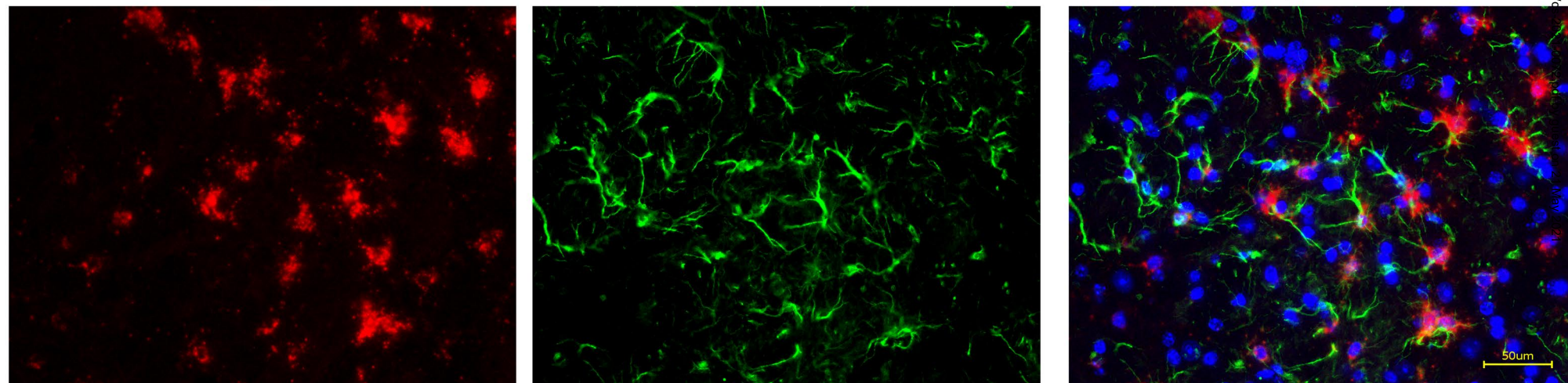
(C) in Agt-Tg. Unaltered HR in saline-heparin filled catheter (B) and telemetry (D) measurements. Telemetry LA estimation (E). 5 days hourly-averaged circadian profile of the HR, MAP and LA in wildtype and Agt-Tg obtained by telemetry (F). Increased maximal pressure response to the ganglionic blocker hexamethonium in Agt-Tg (G). Impaired bradycardia (H) and tachycardia (I) baroreflex control of HR in Agt-Tg. In the bar graphs, values are mean \pm SD for 5-6 animals in each group. * $p < 0.05$; ** $p < 0.01$; *** $p < 0.001$ different from the FVB/N group (Student's *t* test). In the circadian profile, values are the hour average for each parameter \pm SEM for 5 animals in each group. Filled and white intervals below the x axis represent dark and light periods, respectively. MAP = mean arterial pressure, HR = heart rate, LA = locomotor activity.

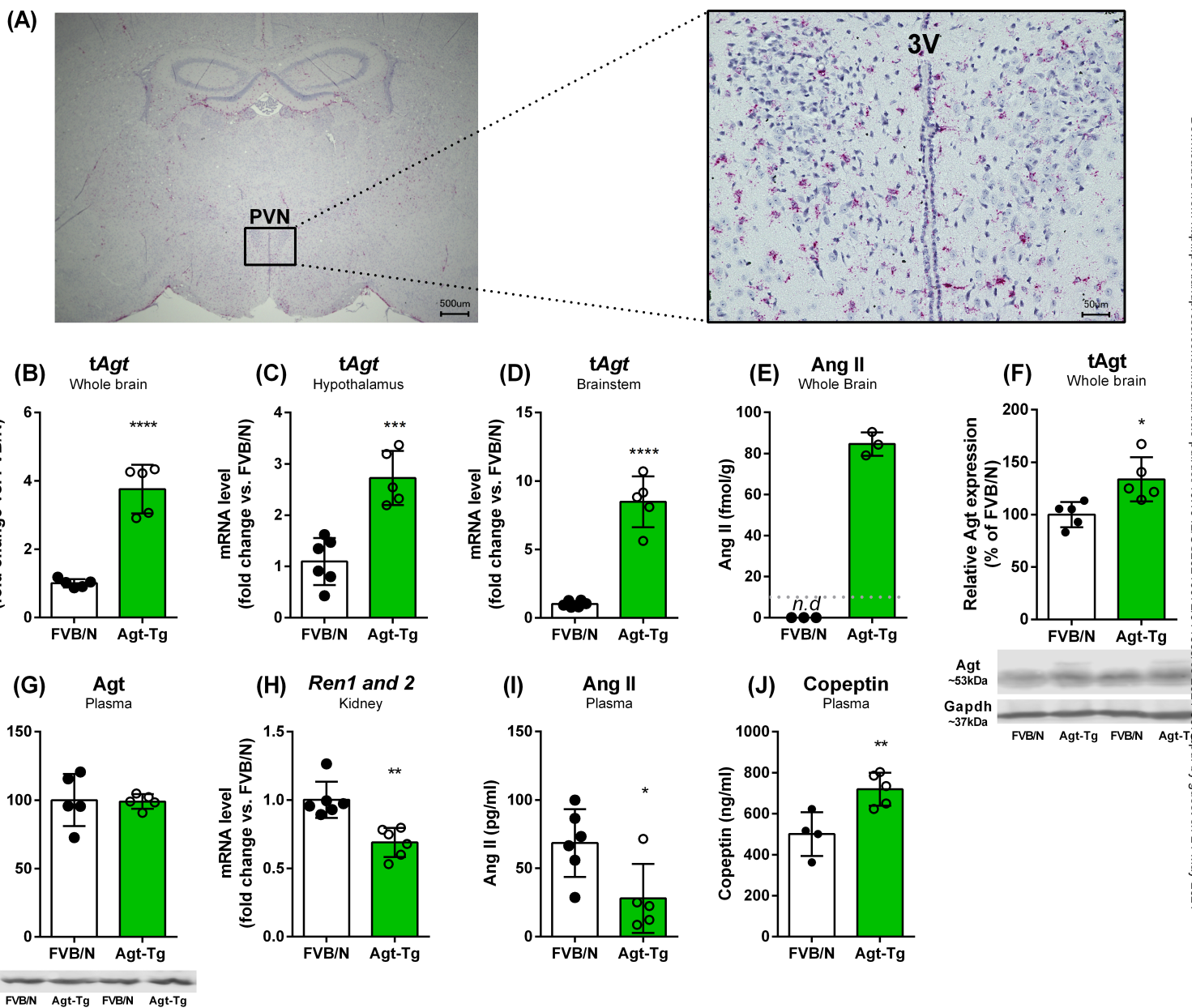
Figure 4 – Brain Ang II and erythropoiesis modulation

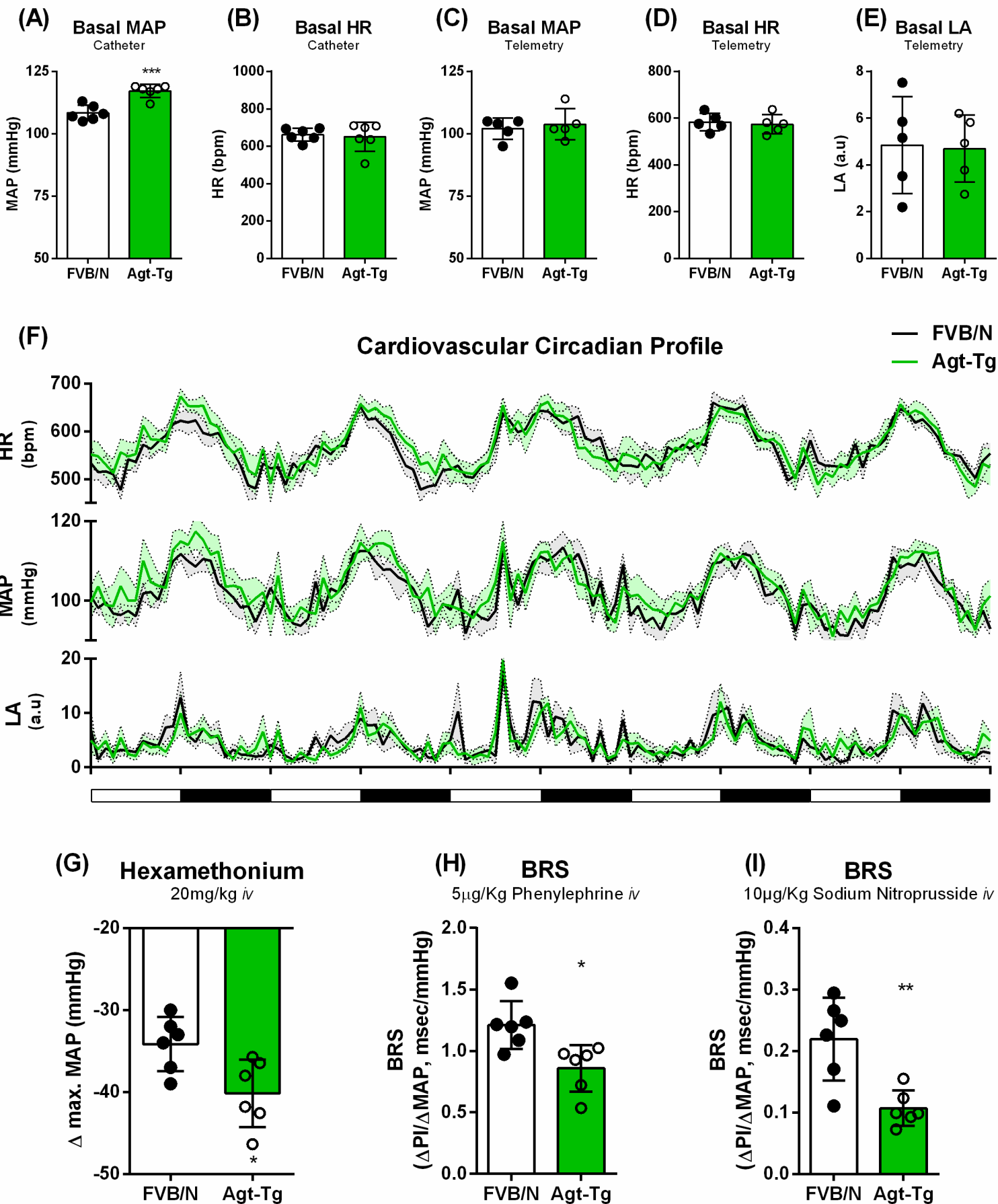
Elevated baseline hematocrit in Agt-Tg (A). Increased baseline RBC (B), HGB (C), and RET (F) and normal MCH (E) in blood of Agt-Tg. Normal renal erythropoietin gene expression in Agt-Tg (D). Sympathectomy normalizes RBC (B), HGB (C) and RET (F) in Agt-Tg. Values are mean \pm SD for 3-6 animals in each group. ** $p < 0.01$ different from the FVB/N group (Student's *t* test). § $p < 0.05$ different from basal FVB/N; ## $p < 0.01$ different from basal Agt-Tg; ££ $p < 0.01$ sympathectomy effect; § $p < 0.05$ interaction between genotype and sympathectomy (two-way ANOVA followed by Tukey's *post hoc* test). RBC = red blood cell, HGB = hemoglobin, MCH = mean corpuscular hemoglobin, RET = reticulocytes.



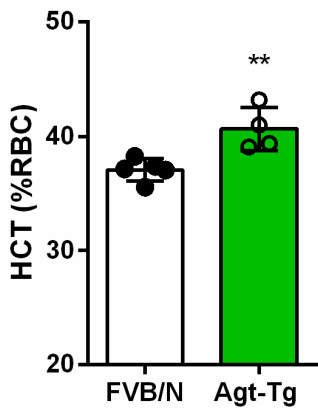
(C) ***Agt*** **GFAP** **Merge - DAPI**



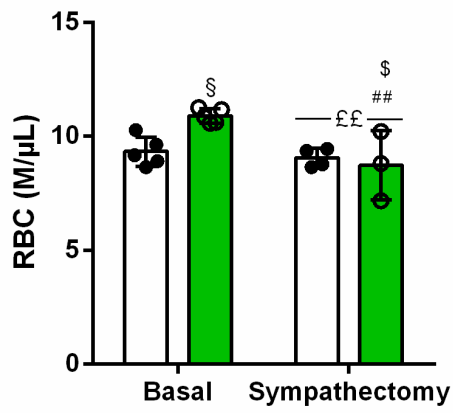




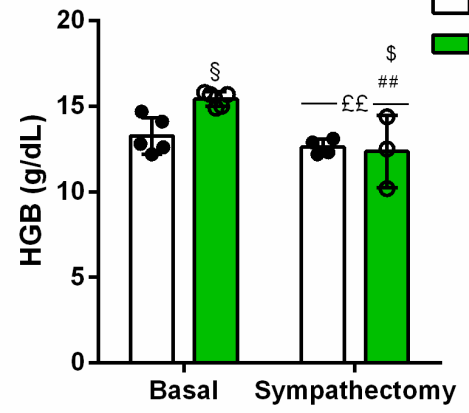
(A) Basal Hematocrit



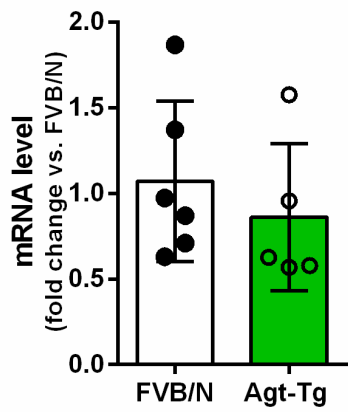
(B) RBC



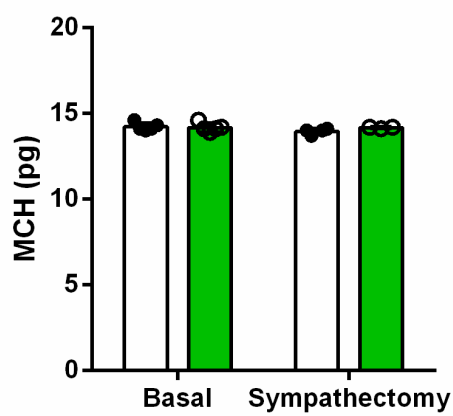
(C) HGB



(D) *Epo*
Kidney



(E) MCH



(F) RET

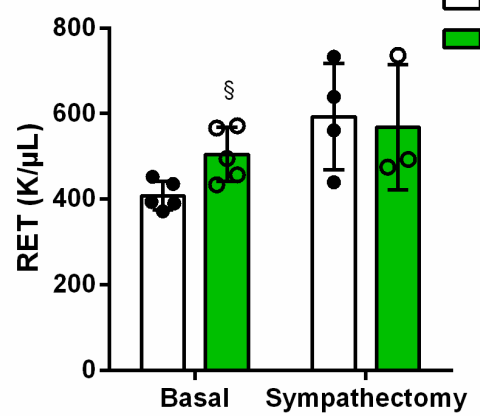


Table 1 – Plasma and urine metabolites.

	Plasma parameters		Urine parameters		
	FVB/N	Agt-Tg	FVB/N	Agt-Tg	
Na ⁺ (mmol/l)	147.6 ± 0.6	148.5 ± 0.8	Na ⁺ (mmol/l)	93.4 ± 39.8	74.7 ± 31.0
K ⁺ (mmol/l)	7.01 ± 0.60	6.51 ± 0.38	K ⁺ (mmol/l)	242.7 ± 45.9	285.5 ± 19.8
TP (g/l)	50.0 ± 1.2	50.0 ± 0.9	ALB (μg/dl)	608.8 ± 68.0	558.6 ± 109.3
ALB (g/l)	25.5 ± 1.4	26.0 ± 0.6	CRE (mg/dl)	30.9 ± 5.6	32.1 ± 4.3
BUN (mg/dl)	26.8 ± 2.3	26.8 ± 1.4	[Na ⁺]/[CRE]	2.99 ± 1.17	2.41 ± 1.04
CRE (mg/dl)	0.12 ± 0.01	0.12 ± 0.01	[K ⁺]/[CRE]	8.11 ± 2.28	9.01 ± 1.36
GLC (mg/dl)	271.3 ± 37.1	259.6 ± 29.3	[ALB]/[CRE]	20.2 ± 3.9	17.7 ± 4.7
Osmolarity (mosmol/kg H ₂ O)	319.9 ± 2.5	320.9 ± 2.8	eUvol. (% of FVB/N)	102.6 ± 17.5	97.6 ± 13.0

Values are mean ± SD for 5-8 animals in each group.

Na⁺ = sodium, K⁺ = potassium, TP = total proteins, ALB = albumin, BUN = blood urea nitrogen, CRE = creatinine, GLC = glucose, [Na⁺] = sodium concentration, [K⁺] = potassium concentration, [ALB] = albumin concentration, [CRE] = creatinine concentration, eUvol. = estimated urinary volume.